



## Research paper

# A No-Reference Blur Metric based on Second-Order Gradients of Image

T. Askari Javaran<sup>1\*</sup>, A. Alidadi<sup>2</sup> and S. R. Arab<sup>2</sup>

1. Faculty of Computer science, Higher Education Complex of Bam, Bam, Iran.

2. Faculty of Computer Engineering, Higher Education Complex of Bam, Bam, Iran.

## Article Info

### Article History:

Received 25 January 2020

Revised 05 August 2020

Accepted 30 November 2020

DOI:10.22044/JADM.2020.9309.2068

### Keywords:

No-reference Blur Metric,

Blur Estimation,

Second-order Gradients.

\*Corresponding

T.askari@bam.ac.ir(T.

Javaran).

author:

Askari

## Abstract

Estimation of the blurriness value in an image is an important issue in the image processing applications such as image deblurring. In this paper, a no-reference blur metric with a low computational cost is proposed, which is based on the difference between the second-order gradients of a sharp image and the one associated with its blurred version.

The experiments, in this work, are performed on four databases including CSIQ, TID2008, IVC, and LIVE. The experimental results obtained indicate the capability of the proposed blur metric in measuring image blurriness and also the low computational cost compared with the other existing approaches.

## 1. Introduction

Blur is a phenomenon that makes the details of an image not clearly visible, and its edges are weakened. In the process of reconstructing a sharp image of its blurry version, an accurate estimation of blur is the first step. Therefore, it is required to define a metric that measures the blurriness value of an image. Several metrics have been introduced for estimation of the blurriness value in an image. However, most of these metrics are based on sophisticated algorithms, and consequently, are time-consuming.

According to the research works, we can say that there are five standard categories of blur metrics. The energy of image can be used in order to estimate the amount of blurriness, because the blur smoothens the image and reduces its energy. This phenomenon is used for image blur estimation in the first category of blur metrics [1]. For blur estimation, in [2], the counted number of high frequency DCT coefficients above a threshold is used. The energy ratio of the high frequency coefficients to the low ones has been used for the estimation of blurriness value in an image in [3]. A blind image blur evaluation has been presented in [4] based on discrete

Tchebichef moments. First, the gradient of a blurred image is computed in order to account for the shape. Then the gradient image is divided into equal-size blocks and the Tchebichef moments are calculated to characterize the image shape. The energy of a block is computed as the sum of squared non-DC moment values. Finally, the proposed image blur score is defined as the variance-normalized moment energy.

The edges of an image have been considered in the second category of blur metrics. In [5], the edges and their width are extracted by vertical and horizontal gradients. In [6], the edges have been extracted by local gradients. The concept of Just Noticeable Blur (JNB) has been employed with the edge detection in [7]. JNB is a perceptual model that specifies the probability of blur detection by the human eye. JNB has been improved by the Cumulative Probability of Blur Detection (CPBD) in [8]. CPBD is based on a probability framework on blur perception sensed by the human eye in different illumination conditions [8]. In [9], the edge information has been extracted by a Toggle operator and used as weight of the local patterns. A support vector

regression method is used to train a predictive model for blur estimation. In [10], the second derivative values along two directions have been combined in order to get the amplitude of the second derivative at the edge point. The ratio of the edge points that have these second derivative amplitudes greater than a particular threshold is calculated as the blurriness value.

The blur metrics in the third category are the statistical methods based on the distribution of the pixel intensities or transform coefficients. The methods proposed in [11,12] use the fact that the sharper images have a greater variance or entropy in their pixel intensities. In [13], the stretch of DCT coefficients distribution has been used as a measure for the estimation of blur. The local phase has coherence in the image discriminating features and therefore the Local Phase Coherence (LPC) has been used to estimate the amount of blur in a given image in [14]. LPC can be extracted from the complex wavelet transform domain. In order to estimate the blurriness value, in [15], the differences between local histograms in a given test image and the blurred version have been used. In [16], a blur metric has been proposed that is based on the difference between discrete cosine transform (DCT) of a sharp image and that of the blurred version. In [17], the shape information has been acquired by computing the gradient map. Then the grayscale image, gradient map, and saliency map are divided into blocks of the same size. The blocks of the gradient map are converted into DCT coefficients, from which the response function of singular values (RFSV) are generated. The sum of RFSV is then utilized to characterize the image blur. In [18], the quality-aware features have been extracted as the gradient of log-likelihood on the natural scene statistics model in order to account for the across space and orientation correlation simultaneously by means of multivariate Gaussian mixture model (GMM). In [19], the spatial and temporal features of image sequences, extracted by convolutional neural networks and long short term memory (LSTM), respectively, have been used to evaluate the degree of image distortion. Then the proposed model is learned to predict the scores of image patches. Finally, a pooling strategy is designed in order to evaluate the quality score of the whole image.

The fourth category of blur metrics are the ones that use the local gradient measures. The Singular Value Decomposition (SVD) has been used to estimate the blurriness value in [20]. In another study, the sharpness value of a given image has been estimated using the relative gradient

intensity corresponding to the two greatest singular values. In [21], a measure has been presented based on a statistical analysis of local edge gradients.

The fifth category of blur metrics are the ones that are provided from a combination of the other measures in four categories. The authors of [22] have proposed a measure based on the total variation in the spatial space (sum of the absolute difference between an image and a spatially shifted version of the image) and the slope of the magnitude spectrum in the frequency space. The total variation represents the gradient of image in the vertical or horizontal direction. Therefore, the total variation is a feature of the fourth category. Also, the slope of the magnitude spectrum in the frequency space is a statistical measure. This statistical measure is based on the distribution of the image transform from the frequency domain. Hence, this feature is in the third category of blur metrics. Indeed, the blur metric proposed in [22] is a combination of the third and fourth categories. The method proposed in [23] is based on both the multi-scale gradients and the wavelet decomposition of the images. Therefore, this blurriness metric is a combination of the third and fourth categories.

In [24], the fuzzy membership of pixels have been obtained via the MC-FCM (Markov Constraints to the Fuzzy-C-Means (MC-FCM)) clustering algorithm, and then, to leverage fuzzy membership from MC-FCM, the blur assessment toward pixels in the edge zone has been provided by modifying the Shannon's entropy. The correlations between the degradations of image qualities and their corresponding hierarchical feature sets have been used for image blur assessment in [25]. The deep residual network, which possesses multiple levels for feature integration, is employed to extract the deep semantics for a high-level visual content representation. By fusing the local structure and the deep semantics, a hierarchical feature set is acquired.

In this paper, an evaluation metric for estimating blurriness in a given image is proposed. The proposed metric is a no reference one, i.e., from an image (without a reference image) estimates the amount of blurriness. This metric is based on a simple feature: if we blur a sharp image with a blur filter, there is a significant difference between the edges of the sharp and blurred versions. The proposed blur metric is based on this difference. The experimental results show that the proposed blur metric can well-estimate the amount of blurriness for various types of blur and images

with different complexities. In addition, it can measure the amount of blurriness with a low time complexity.

The rest of this paper is organized as follows. The proposed blur metric is presented in Section 2. In Section 3, the efficiency of the proposed blur metric is compared with some other existing blur metrics. Finally, we discuss and conclude the proposed method in Section 4.

## 2. Proposed Method

The blurring process makes the details of image not clearly visible and weakens its edges. Suppose that we have a sharp image. If this image is blurred (via a blurring filter), the amount of weakening in its edges is visible and significant. In other words, the difference between the edges of the sharp image and the ones of the blurred version is noticeable and significant.

Now suppose that we blur the same blurry image (via the same blurring filter). The amount of damage on the edges of the blurry image is not very noticeable. In other words, there is not much difference between the edges of a blurred image and its re-blurred version. A sharp image, its blurred version using a low-pass filter, and the re-blurred image using the same filter are presented in figure 1. The edges of these images are also presented. As shown, the difference between the edges of the original and the blurred images is very significant. However, the edges of the blurred and the re-blurred images are not significantly different (at least visually). The mathematical derivations and the concept of blurring and re-blurring an image can be found in [26,27] and [16].

Suppose that we refer to the sharp image as  $f$  the blurred version (via a low-pass filter) as  $g_1$ , and, the re-blurred version (via the same filter) as  $g_2$ . In order to better clarify, we obtained the summation of square difference error (SSDE) between the edges of  $f$  and the edges of  $g_1$ , and between the edges of  $g_1$  and the ones of  $g_2$  for five images chosen from the CSIQ database [28]. The results obtained are plotted in figure 2 in the bar form. SSDE between the edges of the sharp image and the ones of the blurred one is given in blue, and SSDE between the edges of the blurred and re-blurred versions is given in green. As seen, for all the five images, SSDE between the edges of the sharp image and the ones of the blurred version is significantly larger than SSDE between the edges of the blurred and the re-blurred versions.

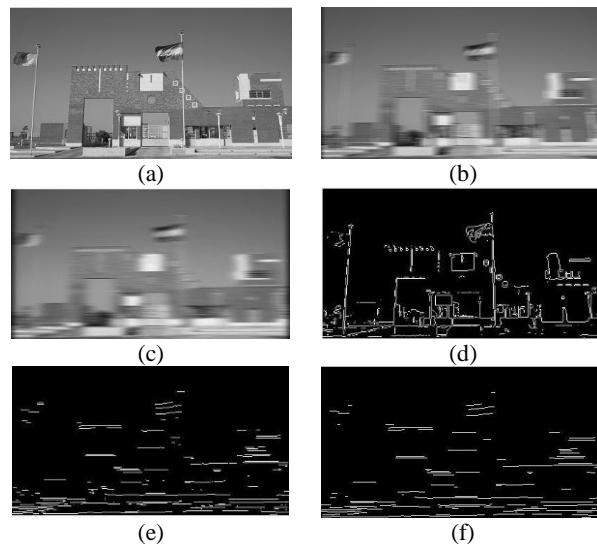


**Figure 1. Difference between the original image and the blurred one: (a) original sharp image; (b) blurred version using a low-pass filter (an average filter with a  $1 \times 15$  window size); (c) re-blurred image using the same filter; (d), (e), and (f) edges of images shown in (a), (b), and (c), respectively.**

This phenomenon is better happened for the second-order edges (gradients) of the images. In figure 3, the second-order edges of the images shown in figure 1(a), (b), and (c) are presented.

In figure 4, we plotted SSDE between the second-order gradients of  $f$  and the second-order gradients of  $g_1$ , and between the second-order gradients of  $g_1$  and the ones of  $g_2$  in the bar form for five images (chosen in Figure 2). As it can be seen, these differences are well-shown for the second gradients.

As it can be seen in figure 3, the number of non-zero second-order edges for the original image is more than those for the blurred one. Due to losing details and weakening edges, a large part of the second-order edges in the blurred image is lost. However, the number of non-zero second-order edges in the blurred and re-blurred images is nearly the same, because only a small part of the other remaining second-order edges is lost in the re-blurred image. As a consequence, we can use the difference between the second-order edges in a given image and the blurred version to introduce a blur metric.

Before introducing the blur metric, the process of calculating the second-order gradients is explained. In order to detect the edge pixels in the given image, first, Canny edge detector is applied to that image. The second derivatives along the horizontal and vertical directions are calculated for all locations in the image that are classified as the edge points.

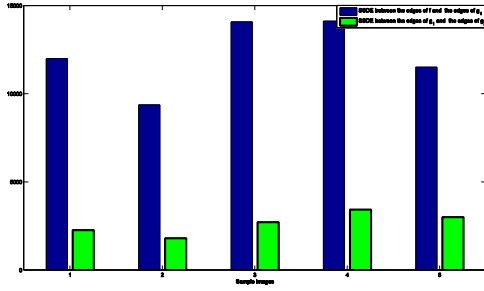


Figure 2. Comparison of SSDE between the edges of the sharp and blurred images and SSDE between the edges of the blurred and re-blurred images for five chosen images (in size of  $512 \times 512$ ) from CSIQ.

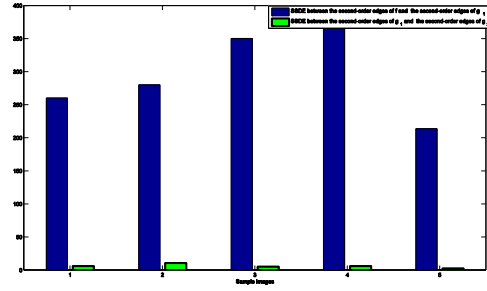
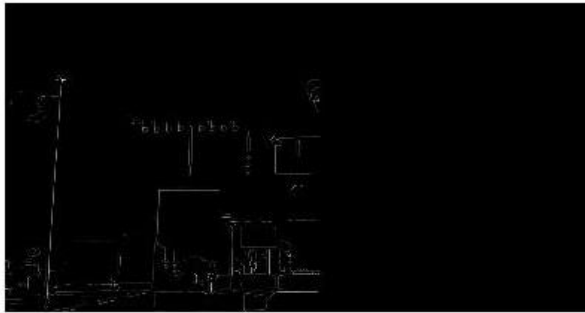
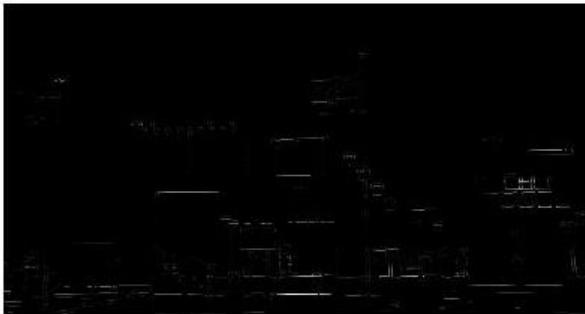


Figure 4. Comparison of SSDE between the second-order edges of the sharp and blurred images and SSDE between the second-order edges of the blurred and re-blurred images for the same five chosen images in Figure 2.



(a)



(b)



(c)

Figure 3. Second-order edges of the images shown in Figure 1(a), (b), and (c).

### 2.1. Blur Metric

For the horizontal case, denoted as the index  $x$ , the second derivative is calculated as:

$$G_{xx}(x, y) = I(x, y) - 2I(x - 1, y) + I(x - 2, y), \quad (1)$$

For the vertical case, denoted as index  $y$ , it is calculated as:

$$G_{yy}(x, y) = I(x, y) - 2I(x, y - 1) + I(x, y - 2), \quad (2)$$

where  $I(x, y)$  represents the pixel value intensity at the edge point location  $(x, y)$ .

In order to get the amplitude of the second derivative at the edge point, the second derivative values along two directions are combined as follows (for all edge points):

$$G(x, y) = G_{xx}(x, y)^2 + G_{yy}(x, y)^2 \quad (3)$$

In order to take the effect of the above-mentioned difference into account (the difference between the second-order edges in a given image and the blurred version), the  $l_1$  norm ratio between the second-order gradients of the given image and those of the blurred version, is suggested as a metric. This blur metric is defined as follows:

$$\beta(I) = \frac{\|G_b\|}{\|G\|}, \quad (4)$$

where  $G_b$  represents the second-order edges of the blurred version of  $I$ , which is obtained by applying a low pass filter on  $I$ .  $\|G\|$  is  $l_1$  norm, and is defined as follows:

$$\|G\| = \sum_{x,y} G(x, y) \quad (5)$$

The blurriness estimated using Eq. 4 is a value within  $[0,1]$ , in which a closer value to 1 indicates that the image is more blurry, and consequently, a closer value to 0 indicates that the image is more sharp. The following is an explanation of this phenomenon.

As mentioned earlier, for a very sharp image, the difference between the second-order gradients of the given image and that of the blurred version is

large. Thus the amount of the fraction denominator is much greater than the fraction face. Therefore, the amount of fraction will be near to 0. As a result, the value of  $\beta$  for a sharp image is close to zero for a sharp image. On the other hand, for a very blurry image, the difference between its second-order gradients and that of the blurred version is small, so the amount of the fraction denominator is not much greater than the fraction face. Hence, the amount of fraction will be near to 1. Consequently, the value of  $\beta$  for a blurry image is close to one.

The blurriness value ( $\beta(I)$ ) of the sharp image shown in figure 1 is about 0.37, whereas, it is about 0.71 for the blurred and 0.87 for the re-blurred ones, shown in figures 1(b) and (c), respectively.

### 3. Experimental Results

We evaluated the performance of the proposed blur metric by applying it to estimate the blurriness of the selected images. We selected four popular databases that contained blurry images: CSIQ [28], TID2008 [29], LIVE [30], and IVC [31]. Each database consists of the original images, distorted versions using Gaussian blurring at different levels. There are 150, 100, 145, and 20 blur images in the CSIQ, TID2008, LIVE, and IVC databases, respectively. The mean opinion scores (MOSs) scores for all the distorted images in all the four databases are presented.

The VQEG report [32] has proposed the suggestions to measure how well the metric values correlate with the provided MOS values and to objectively evaluate its performance. As several researchers have done, we followed these suggestions. In the VQEG report, four indicators are suggested to compute: Spearman's Rank-Order Correlation Coefficient (SRCC), Kendall's Rank-Order Correlation Coefficient (KRCC), Pearson's Linear Correlation Coefficient (PLCC), and Root Mean Squared Error (RMSE). Both SRCC and KRCC are used to validate prediction monotonicity [33].

In order to evaluate the prediction accuracy, PLCC and RMSE are used [33]. If a given measure yields high values in PLCC, SRCC, and KRCC; and low values in RMSE, it will be a good objective quality measure [33]. In [34,35], the definition of these indicators and more details can be found.

The results of the proposed method were compared with those obtained using the most cited no-reference blur metrics: JNBM [7], CPBD

[8], LPC-SI [14], BLINDS-II [36], and NI-DCT [16].

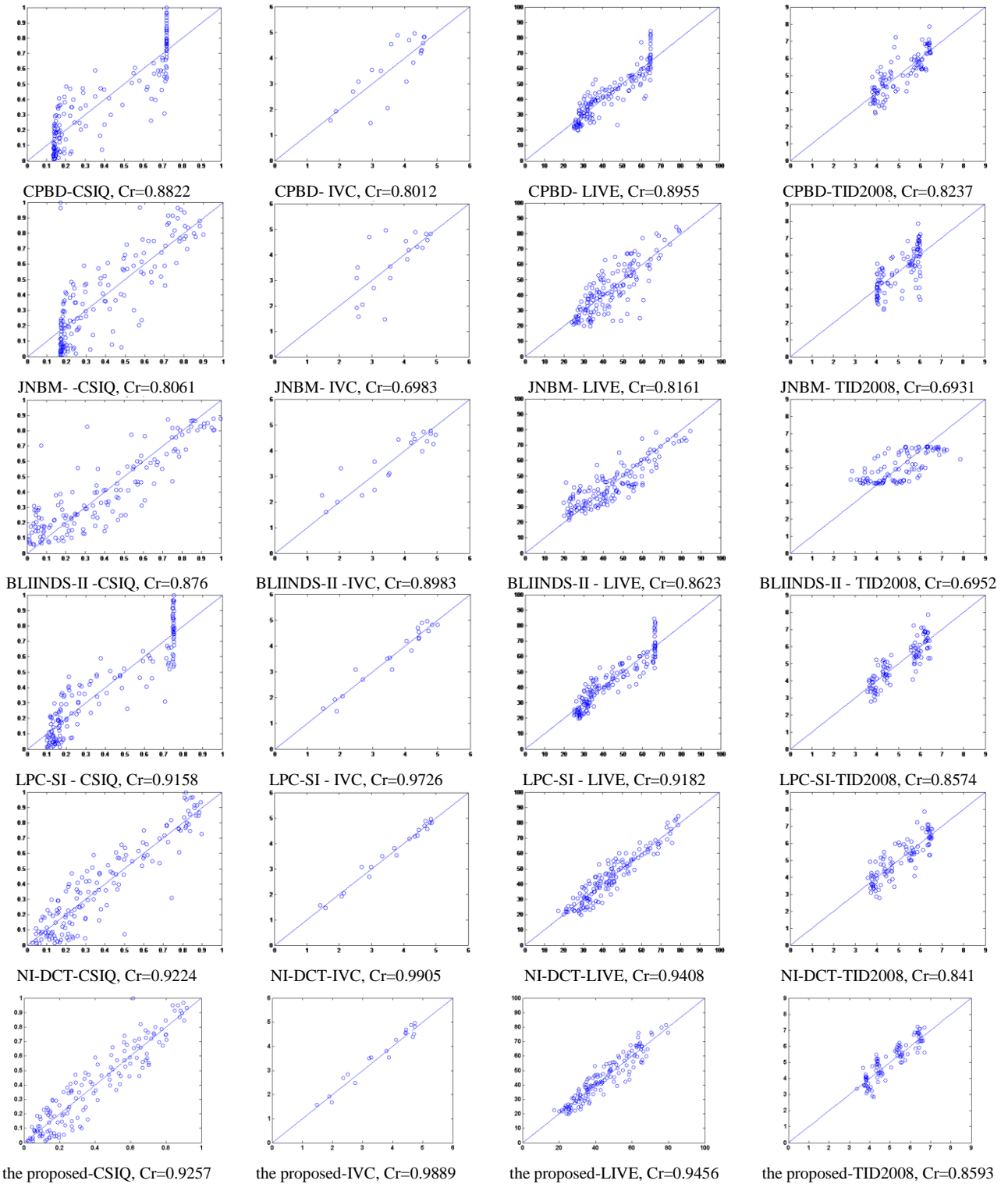
For these six metrics (five above mentioned blur metrics along with the proposed metric), the four indicators introduced earlier were computed. The results obtained are shown in table 1. As it can be concluded, the performance of the proposed blur metric is comparable to the other blur metrics; in some cases, it is the best.

As suggested in the VQEG report, and as done by other researchers, we showed the scatter plots of the MOSs versus the blurriness values estimated by the six blur metrics. This is done for the visual inspection of the correlation between the estimated blurriness values and MOSs. The results obtained are shown in figure 5. In this figure, each sample point represents one test image. As suggested in the VQEG report, a logistic fitting function was used to provide a non-linear mapping between the scores to accommodate for the quality rating compression at the extremes of the test.

As it can be seen, under comparison, the sample points for the proposed blur metric generally tend to be clustered closer to the diagonal lines than the other five blur metrics.

**Table 1. Performance evaluation of the six blur metrics on four databases.**

LIVE (145 blurred images) [30]				
	SRCC	KRCC	PLCC	RMSE
JNBM [7]	0.7876	0.6069	0.8161	9.0857
CPBD [8]	0.9194	0.7653	0.8955	6.9971
BLINDS-II [36]	0.8242	0.6404	0.8623	7.9629
LPC-SI [14]	<b>0.9394</b>	<b>0.7785</b>	0.9182	6.2288
NI-DCT [16]	0.9282	0.7701	0.9408	5.3289
<b>The proposed</b>	0.9322	0.7782	<b>0.9456</b>	<b>5.0234</b>
CSIQ150 (145 blurred images) [28]				
	SRCC	SRCC	SRCC	SRCC
JNBM [7]	0.7624	0.5976	0.8061	0.1669
CPBD [8]	0.8853	0.6646	0.8822	0.1349
BLINDS-II [36]	0.8396	0.709	0.876	0.1382
LPC-SI [14]	<b>0.9071</b>	0.7205	0.9158	0.1151
NI-DCT [16]	0.8888	0.7162	0.9224	0.1107
<b>The proposed</b>	0.8991	<b>0.7214</b>	<b>0.9257</b>	<b>0.1102</b>
IVC (20 blurred images) [31]				
	SRCC	SRCC	SRCC	SRCC
JNBM [7]	0.6659	0.4974	0.6983	0.8172
CPBD [8]	0.769	0.6138	0.8012	0.6832
BLINDS-II [36]	0.8397	0.6667	0.8983	0.5016
LPC-SI [14]	0.9398	0.8042	0.9726	0.2653
NI-DCT [16]	<b>0.9782</b>	<b>0.9101</b>	<b>0.9905</b>	<b>0.1567</b>
<b>The proposed</b>	0.9723	0.9087	0.9889	0.1619
TID2008 (100 blurred images) [29]				
	SRCC	SRCC	SRCC	SRCC
JNBM [7]	0.6667	0.4951	0.6931	0.8459
CPBD [8]	0.8414	0.6301	0.8237	0.6655
BLINDS-II [36]	0.6972	0.4793	0.6952	0.8435
LPC-SI [14]	0.8561	0.6362	0.8574	<b>0.604</b>
NI-DCT [16]	0.833	0.6107	0.841	0.6349
<b>The proposed</b>	<b>0.8565</b>	<b>0.6373</b>	<b>0.8593</b>	0.6076



the proposed-CSIQ, Cr=0.9257      the proposed-IVC, Cr=0.9889      the proposed-LIVE, Cr=0.9456      the proposed-TID2008, Cr=0.8593  
**Figure 5.** Scatter plots between MOSs and the values estimated (after nonlinear mapping) by the six blur metrics over the four blur image databases, with the correlation coefficient (Cr). Top to bottom rows: CPBD [8], JNBM [7], BLIINDS-II [36], LPC-SI [14], NI-DCT [16] and the proposed blur metric; Left to right columns: CSIQ, IVC, LIVE, and TID2008 databases.

In order to compare the runtime of the six blur metrics, another experiment was applied on 150 images with  $512 \times 512$  resolutions from the CSIQ database.

This test was performed on a computer configured with Intel Core i3 CPU 3.60 GHz, 4 GB RAM, Windows 7 64-bit, and MATLAB 8.3. Table 2

shows the runtime of the six blur metrics. Although the BLIINDS-II algorithm is a fast algorithm, it requires a long training process [36]. However, the proposed blur metric is the fastest algorithm.

#### 4. Conclusion and Discussion

In this paper, a metric was proposed for estimating blur in the image. This metric was defined on the basis of the difference between the second-order derivations of the original image and the second-order derivations of the blurred version. If the given image is sharp, there is a significant difference between its second-order derivations and the ones of the blurred version. However, if the image is blurry, this difference is less. This phenomenon is taken to help define a measure of blur. This metric performs better than the other methods. The high speed of this metric is another feature.

**Table 2. Runtime comparisons of blur metrics for images of 512×512 resolution.**

Blur metric	Runtime (second)
JNBM [7]	0.8537
CPBD [8]	0.969
BLINDS-II [36]	0.0853
LPC-SI [14]	2.2763
NI-DCT [16]	0.2027
<b>The proposed</b>	<b>0.0652</b>

#### References

- [1] J. Antkowiak, T. Jamal Baina, F.V. Baroncini, N. Chateau, F. FranceTelecom, A.C.F. Pessoa, F. Philips, "Final report from the video quality experts group on the validation of objective models of video quality assessment," In: *VQEG meeting, Ottawa, Canada*, March, 2000.
- [2] D. B. L. Bong and B. E. Khoo, "An efficient and training-free blind image blur assessment in the spatial domain," *IEICE transactions on Information and Systems*, vol. 97, no. 7, pp. 1864–1871, 2000.
- [3] D. B. L. Bong and B. E. Khoo, "Blind image blur assessment by using valid reblur range and histogram shape difference," *Signal Processing: Image Communication*, vol. 29, no. 6, pp. 699–710, 2014.
- [4] P. Bromiley, "Products and convolutions of gaussian distributions," Medical School, Univ. Manchester, Manchester, UK, Tech. Rep, vol. 3, 2003.
- [5] J. Cavedes and F. Oberti, "A new sharpness metric based on local kurtosis, edge and energy information," *Signal Processing: Image Communication*, vol. 19, no. 2, pp. 147–161, 2004.
- [6] M.-J. Chen and A. C. Bovik, "No-reference image blur assessment using multiscale gradient," *EURASIP Journal on image and video processing*, vol. 2011, no. 1, p. 3, 2011.
- [7] N. N. K. Chern, P. A. Neow, and M. H. Ang, "Practical issues in pixel-based autofocus for machine vision," in *Proceedings 2001 ICRA. IEEE International Conference on Robotics and Automation (Cat. No. 01CH37164)*, vol. 3, pp. 2791–2796, IEEE, 2001.
- [8] S. Chora's, A. Giełczyk, and M. Choraś, "Ten Years of Image Processing and Communications." *International Conference on Image Processing and Communications*. Springer, Cham, 2018.
- [9] S. Erasmus and K. Smith, "An automatic focusing and astigmatism correction system for the sem and ctem," *Journal of Microscopy*, vol. 127, no. 2, pp. 185–199, 1982.
- [10] C. Feichtenhofer, H. Fassold, and P. Schallauer, "A perceptual image sharpness metric based on local edge gradient analysis," *IEEE Signal Processing Letters*, vol. 20, no. 4, pp. 379–382, 2013.
- [11] R. Ferzli, and L. J. Karam, "A no-reference objective image sharpness metric based on the notion of just noticeable blur (jnb)," *IEEE transactions on image processing*, vol. 18, no. 4, pp. 717–728, 2009.
- [12] G. Ghosh Roy, "A Simple Second Derivative Based Blur Estimation Technique," (Doctoral dissertation, The Ohio State University, 2013.
- [13] R. Hassen, Z. Wang, and M. M. Salama, "Image sharpness assessment based on local phase coherence," *IEEE Transactions on Image Processing*, vol. 22, no. 7, pp. 2798–2810, 2013.
- [14] L. He, Y. Zhong, W. Lu, and X. Gao, "A visual residual perception optimized network for blind image quality assessment," *IEEE Access*, vol. 7, pp. 176087–176098, 2018.
- [15] T. A. Javaran, H. Hassanpour, and V. Abolghasemi, "A noise-immune no-reference metric for estimating blurriness value of an image," *Signal Processing: Image Communication*, Elsevier, vol. 47, pp. 218–228, 2016.
- [16] E. C. Larson, and D. M. Chandler, "Most apparent distortion: full-reference image quality assessment and the role of strategy," *Journal of Electronic Imaging*, vol. 19, no. 1, 011006, 2010.
- [17] P. Le Callet, and F. Atrousseau, "Subjective quality assessment ircyn/ivc database: Available: <http://hal.univ-nantes.fr/hal-00580755/>. [Accessed January 10, 2021].
- [18] L. Li, W. Lin, X. Wang, G. Yang, K. Bahrami, and A. C. Kot, "No-reference image blur assessment based on discrete orthogonal moments," *IEEE transactions on cybernetics*, vol. 46, no. 1, pp. 39–50, 2015.
- [19] Q. Li, W. Lin, K. Gu, Y. Zhang, and Y. Fang, "Blind image quality assessment based on joint log-contrast statistics," *Neurocomputing*, vol. 331, pp. 189–198, 2019.
- [20] L. Liu, J. Gong, H. Huang, and Q. Sang, "Blind image blur metric based on orientation-aware local patterns," *Signal Processing: Image Communication*, vol. 80, 115654, 2020.
- [21] X. Marichal, W. Y. Ma, and H. Zhang, "Blur determination in the compressed domain using DCT

- information,” [Conference Proceedings]. In Image processing, 1999. icip 99. proceedings. 1999 international conference on (Vol. 2, p. 386-390). IEEE, 1999.
- [22] P. Marziliano, F. Dufaux, S. Winkler, and T. Ebrahimi, “A no-reference perceptual blur metric,” In Proceedings. International conference on image processing (Vol. 3, pp. III-III), 2002.
- [23] N. D. Narvekar, and L. J. Karam, “A no-reference image blur metric based on the cumulative probability of blur detection (CPBD),” *IEEE Transactions on Image Processing*, vol. 20, no. 9, pp. 2678–2683, 2011.
- [24] E. Ong, W. Lin, Z. Lu, X. Yang, S. Yao, F. Pan, L. Jiang, and F. Moschetti, “A no-reference quality metric for measuring image blur,” in Seventh International Symposium on Signal Processing and Its Applications, 2003. Proceedings., vol. 1, pp. 469–472, IEEE, 2003.
- [25] N. Ponomarenko, V. Lukin, A. Zelensky, K. Egiazarian, M. Carli, and F. Battisti, “Tid2008-a database for evaluation of full-reference visual quality assessment metrics,” *Advances of Modern Radioelectronics*, vol. 10, no. 4, pp. 30–45, 2009.
- [26] M. A. Saad, A. C. Bovik, and C. Charrier, “Blind image quality assessment: A natural scene statistics approach in the dct domain,” *IEEE transactions on Image Processing*, vol. 21, no. 8, pp. 3339–3352, 2012.
- [27] D. Shaked, and I. Tastl, “Sharpness measure: Towards automatic image enhancement,” In IEEE international conference on image processing 2005 (Vol. 1, pp. I-937), 2005
- [28] H. Sheikh, “Live image quality assessment database release 2,” Available: <http://live.ece.utexas.edu/research/quality>, [Accessed January 10, 2021].
- [29] H. R. Sheikh, M. F. Sabir, and A. C. Bovik, “A statistical evaluation of recent full reference image quality assessment algorithms,” *IEEE Transactions on image processing*, vol. 15, no. 11, pp. 3440–3451, 2006
- [30] C. T. Vu, T. D. Phan, and D. M. Chandler, “S3: A spectral and spatial measure of local perceived sharpness in natural images,” *IEEE transactions on image processing*, vol. 21, no. 3, pp. 934–945, 2011
- [31] J. Wu, J. Zeng, W. Dong, G. Shi, and W. Lin, “Blind image quality assessment with hierarchy: Degradation from local structure to deep semantics,” *Journal of Visual Communication and Image Representation*, vol. 58, pp. 353–362, 2019.
- [32] S. Xu, S. Jiang, and W. Min, “No-reference/blind image quality assessment: a survey,” *IETE Technical Review*, vol. 34, no. 3, pp. 223–245, 2017.
- [33] Y. Xu, W. Zheng, J. Qi, and Q. Li, “Blind image blur assessment based on markov-constrained fcm and blur entropy,” In 2019 IEEE international conference on image processing (ICIP) (pp. 4519–4523), 2019.
- [34] S. Zhang, P. Li, X. Xu, L. Li, and C. C. Chang, “No- reference image blur assessment based on response function of singular values,” *Symmetry*, vol. 10, no. 8, 304, 2018.
- [35] E. Fadaei-Kermani, G. Barani, M. Ghaeini-Hessaroeyeh, “Drought Monitoring and Prediction using K-Nearest Neighbor Algorithm,” *Journal of AI and Data Mining*, vol. 5, no. 2, pp. 319-325. doi: 10.22044/jadm.2017.881, 2017.
- [36] X. Zhu, and P. Milanfar, “A no-reference sharpness metric sensitive to blur and noise,” In 2009 international workshop on quality of multimedia experience (pp. 64–69), 2009.

## ارائه یک معیار بدون مرجع برای تخمین تاری در تصویر بر اساس گرادیان‌های مرتبه دوم

طیبه عسکری جواران<sup>۱\*</sup>، امیر علیدادی<sup>۲</sup> و سعیدرضا عرب<sup>۳</sup>

<sup>۱</sup> گروه علوم کامپیوتر، مجتمع آموزش عالی بم، بم، ایران.

<sup>۲</sup> گروه مهندسی کامپیوتر و فناوری اطلاعات، مجتمع آموزش عالی بم، بم، ایران.

ارسال ۱۳۹۸/۱۱/۰۵ بازنگری: ۱۳۹۹/۰۵/۱۵ پذیرش ۱۳۹۹/۰۹/۱۰

---

### چکیده:

تخمین مقدار تاری در تصویر مسئله مهمی در کاربردهای پردازش تصویر مانند رفع تاری تصویر است. در این مقاله، یک معیار تاری بدون مرجع با هزینه محاسباتی کم ارائه شده است که براساس تفاوت بین گرادیان‌های مرتبه دوم یک تصویر واضح و گرادیان‌های مرتبه دوم در نسخه تار شده آن استوار است. آزمایش‌های صورت گرفته در این مقاله بر روی چهار پایگاه داده شامل CSIQ، TID2008، IVC و LIVE انجام شده است. نتایج آزمایشی نشان‌دهنده توانایی معیار تاری پیشنهادی در اندازه‌گیری تاری تصویر، همچنین هزینه محاسباتی پایین، در مقایسه با سایر روش‌های موجود است. **کلمات کلیدی:** معیار تاری بدون مرجع، تخمین تاری، گرادیان‌های مرتبه دوم.

---